Crystal structure of the carbapenemase OXA-24 reveals insights into the mechanism of carbapenem hydrolysis

Elena Santillana*, Alejandro Beceiro†, Germán Bou†, and Antonio Romero*‡

*Departamento de Estructura y Función de Proteínas, Centro de Investigaciones Biológicas, Consejo Superior de Investigaciones Cientificas, Ramiro de Maeztu 9, E-28040 Madrid, Spain; and †Servicio de Microbiología-Unidad de Investigación, Complejo Hospitalario Universitario Juan Canalejo, As Xubias 84, E-15006 La Coruña, Spain

Edited by Gregory A. Petsko, Brandeis University, Waltham, MA, and approved February 9, 2007 (received for review August 31, 2006)

Combating bacterial resistance to β-lactams, the most widely used antibiotics, is an emergent and clinically important challenge. OXA-24 is a class D β-lactamase isolated from a multiresistant epidemic clinical strain of *Acinetobacter baumannii*. We have investigated how OXA-24 specifically hydrolyzes the last resort carbapenem antibiotic, and we have determined the crystal structure of OXA-24 at a resolution of 2.5 Å. The structure shows that the carbapenem's substrate specificity is determined by a hydrophobic barrier that is established through the specific arrangement of the Tyr-112 and Met-223 side chains, which define a tunnel-like entrance to the active site. The importance of these residues was further confirmed by mutagenesis studies. Biochemical and microbiological analyses of specific point mutants selected on the basis of structural criteria significantly reduced the catalytic efficiency (k_{cat}/K_m) against carbapenems, whereas the specificity for oxacillin was noticeably increased. This is the previously unrecognized crystal structure that has been obtained for a class D carbapenemase enzyme. Accordingly, this information may help to improve the development of effective new drugs to combat β-lactam resistance. More specifically, it may help to overcome carbapenem resistance in *A. baumannii*, probably one of the most worrying infectious threats in hospitals worldwide.

β-lactamases | carbapenem resistance | enzyme mechanism | protein crystallography | *Acinetobacter baumannii*

Bacteria hydrolyze β-lactam antibiotics primarily by using β-lactamases in an acylation–deacylation-based process. By inactivating peptidoglycan transpeptidases, members of the family of penicillin-binding proteins, β-lactam antibiotics have been successfully used for many years to inhibit the peptidoglycan synthesis responsible for the biosynthesis of the bacterial cell wall (1, 2).

β-lactamases can be divided into four classes (A, B, C, and D) according to their sequence similarities (3). On the basis of their different catalytic mechanisms, two groups have been established whereby class B enzymes are metalloproteins that require zinc for their activity, and class A, C, and D β-lactamases contain serine groups in their active site (4). Oxacillinases are Ambler class D β-lactamases with hydrolytic activity against penicillins, extended-spectrum cephalosporins, methicillin, and aztreonam (5).

Recently, a new type of oxacillinases with carbapenemase activity has been identified in different parts of the world (6–11). In contrast to the other oxacillinases, most of these new OXA-type carbapenemases lack hydrolytic activity against oxacillin, cloxacillin, and methicillin, and they display resistance to carbapenems (9, 12). Based on their amino acid sequence, these OXA-type carbapenemases can be grouped into eight different clusters (13). Moreover, these enzymes have been seen to be widely dispersed in some clinically relevant species, such as *Acinetobacter baumannii* (where four groups have been identified: OXA-23, OXA-24, OXA-51, OXA-58, and their variants) and *Pseudomonas aeruginosa* (OXA-50 family; ref. 13). Carbapenems are the remaining drug of choice to treat these multiresistant pathogens, which may be responsible for severe nosocomial infections. Hence, the emergence of OXA-type carbapenemases raises a particularly disturbing problem (12, 14).

The structures of class A and C β-lactamases, as well as that of the prototypic class D oxacillinases (OXA-1, OXA-2, OXA-10, and OXA-13), have been determined (15–19). Comparison of these active-serine enzymes has identified similarities in their overall folding involving one helical and one mixed α/β domain and three highly conserved active site elements in a cleft located between the two domains that are involved in hydrolysis. Despite these similarities, important differences both adjacent to the active site and in the omega loop region may establish their specific hydrolytic profiles (17, 18). However, no structures of a class D carbapenemase are currently available.

Here, we present a previously unrecognized three-dimensional structure describing a class D carbapenem-hydrolyzing oxacillinase, OXA-24, extracted from a clinically epidemic multidrug-resistant *A. baumannii* strain (9). In combination with mutagenesis, biochemical experiments, and modeling, these data suggest a plausible mechanism that may be associated with carbapenem hydrolysis of a class D carbapenemase enzyme. Moreover, our structural and biochemical studies provide the molecular basis to explain the acquisition of carbapenem specificity. Together this information could serve as a starting point for the development of new antimicrobial agents given that there is clearly a specific need for a potent class D β-lactamase inhibitor to bridge the existing therapeutic void.

Results

Overall Folding. The approximate dimensions of OXA-24 are 58 × 46 × 38 Å, and structurally it involves an α/β fold where the helices are exposed to the solvent surrounding the core of the central β-sheet (Fig. 1*a*). The molecule can be separated into two domains, one helical and one of a mixed α/β structure containing a central six-stranded antiparallel β-sheet. The N- and C-terminal helices (α1 and α9) can be found on one side of this β-sheet, and there is a single 3_{10} helix (α3) on the other. The active site has an overall positive charge, and it lies between the interface of the β-sheet and the helical subdomain, adopting the appearance of an extended cleft (Fig. 1*b*). The catalytic-binding pocket is formed by the β4 strand together with the N-terminal end of the 3_{10} α3 helix and the

Author contributions: E.S. and A.B. contributed equally to this work; G.B. and A.R. designed research; E.S. and A.B. performed research; E.S., A.B., G.B., and A.R. analyzed data; and E.S., G.B., and A.R. wrote the paper.

The authors declare no conflict of interest.

This article is a PNAS Direct Submission.

Abbreviations: MIC, minimal inhibitory concentration; DM, double mutant.

Data deposition: The atomic coordinates have been deposited in the Protein Data Bank, www.pdb.org (PDB ID code 2JC7).

‡To whom correspondence should be addressed. E-mail: romero@cib.csic.es.

This article contains supporting information online at www.pnas.org/cgi/content/full/0607557104/DC1.

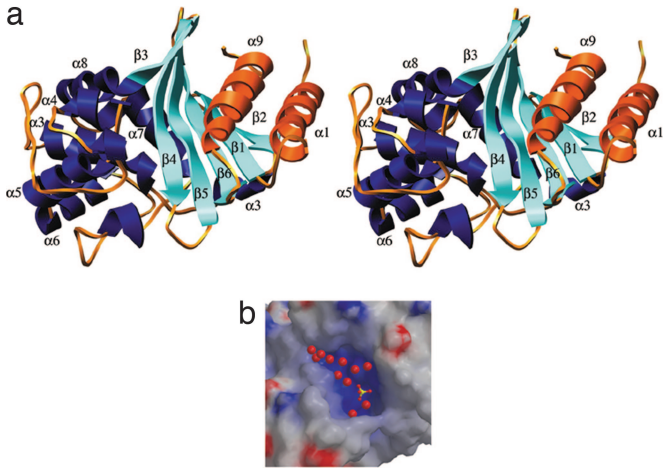

Fig. 1. Structure of OXA-24, a class D carbapenem-hydrolyzing oxacillinase. (*a*) Stereodiagram showing the overall folding of OXA-24 with the two domains colored differently: the α helical domain is shown in navy blue and in the mixed α/β domain, the β-sheet is shown in cyan, and the α-helices are shown in orange. (*b*) Surface potential of the tunnel-like entrance to the active site, where blue is positive and red is negative. The sulfate ion and water molecules are shown in ball-and-stick mode.

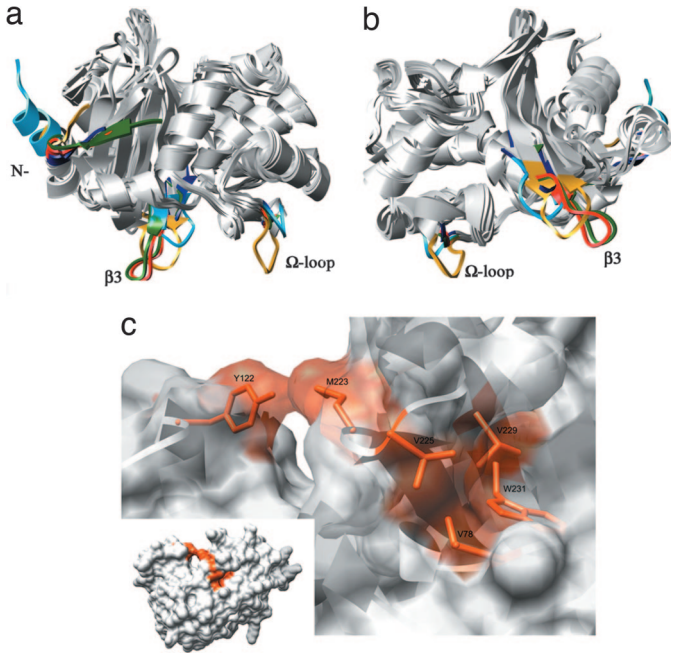

Fig. 2. Details of the structure of OXA-24. (*a* and *b*) Selected views of the superposition of OXA-24 (cyan) and the oxacillinase members of class D β-lactamases of known structure, OXA-1 (yellow), OXA-2 (navy blue), OXA-10 (red), and OXA-13 (green), highlighting the major structural differences. OXA-24 displays an elongated α-helix (α1) at the N terminus and the β3 strand implicated in dimerization in other oxacillinases is directed toward the C-terminal helix (α9). Important differences can also be observed in the Ω-loop. (*c*) Detail of the nonpolar region at the lower border of the active binding cleft. The hydrophobic core formed by several nonpolar residues (Val-78, Val-225, Val-229, and Trp-231) contributes to the stability of the solvent-exposed β4-β5 loop and partially blocks the access to the bottom part of the cleft.

loop between the α4 and α5 helices. In the absence of substrate, the cavity is filled by a sulfate ion and a network of water molecules, thereby providing a set of contact points that can be encountered upon antibiotic accommodation.

The structure displays an overall organization very similar to that found in other class A, C, and D β-lactamases (15–19), as well as in other DD-transpeptidases (20, 21). For example, the rms difference in the atomic positions for the common C^{α} residues of OXA-24 is 1.3 Å (225 C^{α} atoms) when compared with that of the oxacillinase class D β-lactamase OXA-10 (17, 19) and 2.4 Å (169 C^{α} atoms) when compared with a typical class A enzyme (*Escherichia coli* TEM-1; ref. 22). The nucleus of the β-sheet and almost all of the adjacent α-helices (α1, α3, and α5 to α9) can be readily superimposed when considering this group of active-serine enzymes [supporting information (SI) Fig. 6 *a* and *b*] (23). However, despite the high degree of similarity mentioned above, a number of differences with respect to the overall folding may contribute to the particular specificity for β-lactam as well as variations in regions adjacent to the active site (24).

Structural Homology to the Class D Oxacillinase Family. Protein folding is thought to be well conserved between OXA-24 and the oxacillinase members of class D β-lactamases with defined structures, namely the following: OXA-1 from *E. coli* (15), OXA-2 from *Salmonella typhimurium* (PDB ID code IK38), and both OXA-10 and OXA-13 from *Pseudomonas aeruginosa* (17–19). Although the sequence identity with other members of the oxacillinase family only ranges from 23% with OXA-1 to 39% with OXA-10, the position of the secondary structural elements in the helical and the mixed α/β domains are highly conserved in OXA-24. However, significant differences were observed in several regions of OXA-24 when compared with other OXA structures. For example, the biggest difference was observed at the N terminus (Fig. 2*a*), which exhibits an elongated α-helix (α1) in OXA-24 instead of the common β1/α1 motif present in the oxacillinase family. In this respect, OXA-24 closely resembles the N terminus of the TEM-type class A β-lactamases (Fig. 6*b*; ref. 22).

The relative orientation of the short β3 strand at the top of the binding site, directly implicated in dimerization, is different from the topologically equivalent strand of the three dimeric oxacillinases [OXA-2 (PDB ID code IK38), -10, and -13; refs. 17–19]. However, it is similar to that observed in the monomeric OXA-1 structure (15). Hence, the β3 strand is bent ≈30° inward when compared with its position at the equivalent dimerization interface in the oxacillinase family. Thus, it is directed toward the C-terminal helix (α9), disrupting a set of potentially favorable interactions and thereby interfering with dimer formation. Size exclusion chromatography and analytical centrifugation showed that OXA-24 exists exclusively as a monomer at concentrations between 0.1 and 100 μM.

A further interesting difference that was observed at the lower border of the active binding cleft involves the loop connecting the β4 and β5 strands (Fig. 2*b*). Maximum displacement was observed at residue Gly-224, which in comparison with the corresponding loop from the OXA structures is shifted toward the center of the binding groove in the direction of the Ω-loop (4.6 Å in OXA-1 and 6.8 Å in OXA-10; refs. 15, 17, and 19). Moreover, the movement of the β4-β5 loop in OXA-24 partially blocks the bottom part of the groove in the cleft. Because of the lateral chains of several nonpolar residues (Val-78, Val-225, Val-229, and Trp-231), this movement probably creates a hydrophobic core, thereby contributing to the stability of the solvent-exposed loop (Fig. 2*c*). This dynamic behavior nourished the assumption that the movements of these loops may determine the specificity of distinct OXA variants for diverse β-lactams (23).

The β-Lactam Active Site. The OXA-24 β-lactam active site is readily discernible at the junction of the two domains (Fig. 1*a*). In agreement with previous studies (17–21), it comprises residues from the β4 strand together with those coming from the N-terminal end of the 3_{10}-helix α3 and a number of residues from the loop between helices α4 and α5 (Fig. 3*a*). This region includes three common

BIOCHEMISTRY

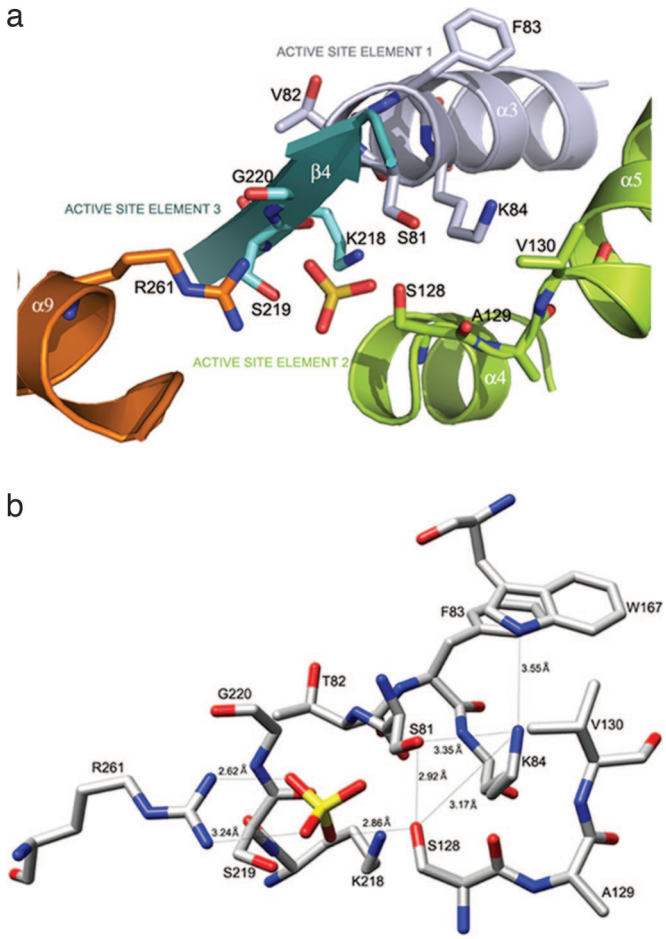

Fig. 3. Close-up view of the β-lactam active site in OXA-24. (*a*) Representation of the active site elements (17). The first element (gray) is located at the N-terminal end of the 3_{10}-helix α3, and it is formed by residues Ser-81-Thr-82-Phe-83-Lys-84. The second motif (green), Ser-128-Ala-129-Val-130, lies in the loop connecting helices α4 and α5. The third active site element (cyan) is formed by the residues Lys-218-Ser-219-Gly-220 from the β4 strand. (*b*) Detailed interactions showing the contact network at the active site (shown as solid lines).

motifs that converge to form the active site, and these are referred to as the active site elements (17).

The first of these elements lies at the N-terminal end of the 3_{10}-helix α3, and it is formed by residues Ser-81-Thr-82-Phe-83-Lys-84. This element contains the catalytic serine residue Ser-81, which acts as the nucleophile in the acylation step of the reaction (17). Indeed, together with Lys-84 this residue is included in the first of the three signature sequences conserved within penicillin-binding proteins/β-lactamases, the Ser-X-X-Lys motif (25). As well as establishing contacts with water molecules in the cleft, the hydroxyl group of Ser-81 establishes a weaker hydrogen bond with the N^{ζ} of Lys-84 (3.35 Å) than that observed in other oxacillinases (2.9 Å in OXA-10; ref. 17). The relative weakness of this interaction is compensated by a slight movement of Lys-84 within the crevice, pointing to the Ω-loop, which forms a hydrogen bond with the side chain nitrogen of the conserved Trp-167 (3.55 Å, Fig. 3*b*).

The second active site element in class D β-lactamases lies in the loop connecting α4 and α5 helices, and it is represented by the conserved motif Ser-128/X/Val-Ile (Fig. 3*a*). The lateral hydroxyl chain of Ser-128 is accommodated in the direction of the active-serine Ser-81, forming hydrogen bonds with the neighboring residues: O^{γ} Ser-128—O^{γ} Ser-81 (2.92 Å), O^{γ} Ser-128—N^{ζ} Lys-84 (3.17 Å), and O^{γ} Ser-128—O SO_4 (2.86 Å, Fig. 3*b*). Accordingly, the hydrogen bond network associated with Ser-128 presents subtle differences with that of the rest of the oxacillinase family. A further characteristic feature within this second element is the presence of a nonpolar residue (Val-130), which is unique to class D enzymes (5). The nonpolar side chain of Val-130 may contribute to the broad substrate specificity of the class D enzymes. Indeed, not only is this side chain a major determinant for cleaving substrates with bulkier side groups (i.e., the isoxazolyl moiety of oxacillins), but it also participates in hydrophobic rather than hydrogen bonding interactions (17, 19, 26). Moreover, recent studies on clinical isolates of carbapenem multiresistant *A. baumannii* reveal a new subgroup in the OXA carbapenemase family (27). As observed in OXA-51 (10), all enzymes of the novel subgroup 3 carbapenem-resistant *A. baumannii* had a conserved valine to isoleucine substitution in the second element of the active site S-X-V.

Several residues from the β4 strand form the upper part of the cleft, which runs horizontally from left to right and includes the conserved Lys-218-Ser-219-Gly-220 sequence of the third active site element (Lys/X/Gly consensus sequence, Fig. 3*a*; ref. 25). The conformation of this segment is virtually identical to the Lys-205-Thr-206-Gly-207 component of the oxacillinase class D β-lactamases. Notably, this region has also been shown to be essential for the binding of the carboxylate group of β-lactam antibiotics in penicillin-binding proteins and in class A and D β-lactamases (28, 29). Moreover, the guanidinium group of Arg-261 protruding from the α9 helix is located in an area similar to Arg-250 in OXA-10 (17). In OXA-10, this group interacts with a sulfate ion in the active site, resembling the carboxylate group of the substrate in the x-ray structures of acyl-enzyme complexes (28, 29). Thus, the fact that there is close structural similarity between the β-lactam active site of OXA-24 and the oxacillinases strongly suggests that the hydrolytic mechanism used by OXA-24 is similar to that of other class D β-lactamases (25).

The differences at the β-lactam active site in OXA-24 are subtle. Nevertheless, despite the overall similarity in folding, significant differences must arise between OXA-24, a class D oxacillinase with carbapenemase activity, and structurally related oxacillinases to account for the functional differences (i.e., its hydrolytic activity toward carbapenems as well as its apparent lack of activity against oxacillin).

Molecular Basis for Carbapenem Specificity. The three common motifs around the active site that are important for enzyme activity were identified in structural studies on both native oxacillinases (15–17, 19) and when it exists in a complex with meropenem and imipenem (18). Moreover, the mechanism by which class D β-lactamases hydrolyze β-lactam antibiotics is thought to be slightly different from that observed in class A and C enzymes (17). However, as recently pointed out (13), the structural information currently available does not enable us to define structure/function relationships that might help us to understand the mechanisms associated with carbapenem hydrolysis in the OXA-type carbapenemases. Likewise, we are unable to identify the key residues that modulate this specificity.

Nevertheless, by more closely examining the molecular surface of the active site, the entrance to the cleft of OXA-24 differs significantly from that of OXA-10, a representative member of the oxacillinase family (Fig. 4 *a* and *b*). Indeed, direct hydrophobic interactions orchestrate a specific arrangement of the Tyr-112 and Met-223 side chains to create a hydrophobic barrier. To some extent this barrier restricts access to the cleft, defining a tunnel-like entrance to the active site. This hydrophobic environment over the active site is stabilized by other hydrophobic contacts, for example, those of Thr-111, Trp-115, and Trp-221, thereby contributing to the stability of the nonpolar interface.

The tunnel has a diameter of ≈6.3 Å, which permits it to directly regulate the shape and chemical nature of the antibiotics that can access the active site before catalysis and those that may reach the

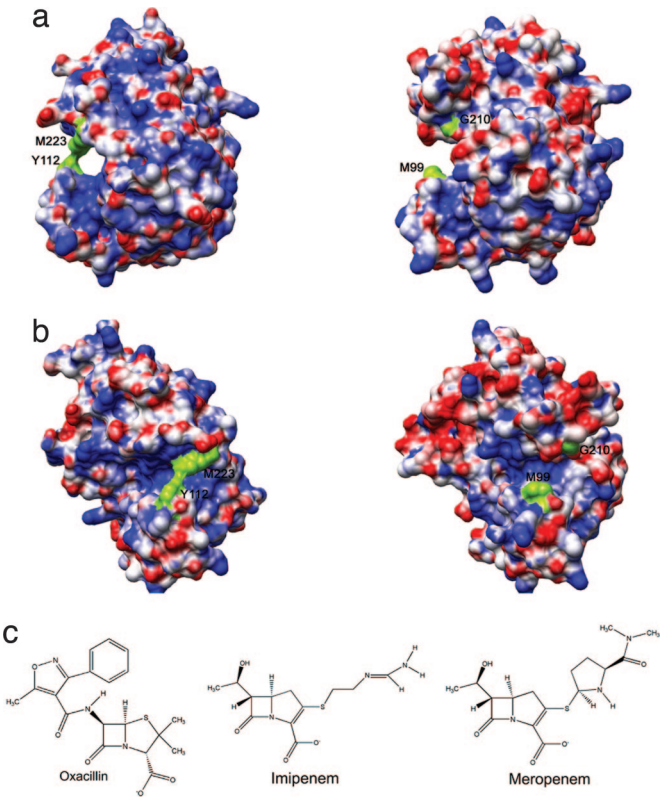

Fig. 4. Acquisition of carbapenem specificity in OXA-24. (*a* and *b*) Surface potential drawing in two different orientations of OXA-24 (*Left*) and OXA-10 (*Right*) with positive and negative-charged regions shown in blue and red, respectively. Residues Tyr-112 and Met-223 and their structural equivalents in OXA-10, Met-99, and Gly-210 are colored green. The relative orientation of both key residues in OXA-24 (*Left*) specifically delimits access to the catalytic binding site, whereas the cleft is fully open in OXA-10. (*c*) Chemical structures of indicated antibiotics.

catalytic Ser-81 residue. A comparison of the chemical structures of oxacillin and the carbapenems, imipenem, and meropenem (Fig. 4*c*) should further elucidate how the selective hydrolytic behavior of OXA-24 arises. The bulky methylphenylisoxazolyl moiety of the oxacillin molecule is located at the left position of the β-lactam ring. Therefore, access of this substrate to the active site in the wild-type (WT) OXA-24 enzyme may be difficult, because of both steric restrictions and the architecture of the catalytic binding site. Interestingly, this feature may account for the relatively lower activity of OXA-24 toward this antibiotic when compared with other oxacillinases ($k_{cat}/K_m \approx 200\ mM^{-1}\ s^{-1}$). On the other hand, the small size of the hydroxyethyl moieties of imipenem and meropenem and the hydrophobic character of the tunnel-like channel are suitable to accommodate carbapenems, in accordance with the substrate affinity of OXA-24. Accordingly, we investigated the effect that point mutations of Tyr-112 and Met-223 had on substrate selectivity in *A. baumannii*.

Table 1. Antibiotic MIC values (μg/ml) determined for *A. baumannii OXA-24 WT and selected structure-based mutants**

Antibiotic	WT OXA24	Y112A	M223A	OXA-24 DM	pAT-RA†
Ampicillin	>256	>256	>256	>256	>256
Imipenem	32	4	16	4	0.5
Meropenem	64	1	16	0.5	0.25

**A. baumannii* transformed with pAT-RA with the corresponding gene and expressing OXA-24 WT or that with the indicated amino acid replacements.
†*A. baumannii* harboring solely pAT-RA as negative control. MICs were determined in the presence of 50 μg/ml rifampin. Identical MICs were obtained with three different transformants in each case.

Point Mutants That Altered Substrate Selectivity. The minimal inhibitory concentration (MIC) values of *A. baumannii* JC7/04 expressing either WT OXA-24 or its single or double mutants are shown in Table 1. Because the *A. baumannii* host is intrinsically resistant to most β-lactam antibiotics (with the exception of carbapenems), the susceptibility to ampicillin and oxacillin can be measured only by kinetic experiments with purified OXA-enzymes. With carbapenems, clear imipenem and meropenem resistance was observed (following NCCLS breakpoints) when the WT OXA-24 was expressed in *A. baumannii* (Table 1), yielding MIC values of 32 and 64 μg/ml, respectively. In contrast to the M223A substitution that slightly decreased the carbapenem MIC values (Table 1), the Y112A mutation diminished both the imipenem and meropenem MIC values to 4 and 1, respectively (NCCLS susceptibility breakpoints were established as $\leq$4 μg/ml). When both amino acid changes were introduced into WT OXA-24 together to produce the OXA-24 double mutant (DM), the MIC for imipenem decreased to 4 μg/ml, whereas meropenem practically reached the basal levels found in *A. baumannii* with the pAT-RA plasmid (negative control).

To further clarify the role of the Tyr-112 and Met-223 residues in the carbapenemase activity of OXA-24, biochemical experiments were carried out using purified WT OXA-24, OXA-24-Y112A (because this substitution seemed more important than M223A), and the OXA-24 DM (the overall kinetic results from these experiments are shown in Table 2). With regard to ampicillin, the k_{cat}/K_m ratio was three to six times lower in both OXA-24 mutants than in WT OXA-24. Indeed, although k_{cat} was similar in each of the three proteins, the K_m was clearly higher for the mutated enzymes. Thus, the reduced catalytic efficiency against ampicillin in

Table 2. Kinetic parameters of WT OXA-24 and its mutants toward the indicated antibiotics*

	Ampicillin			Oxacillin			Imipenem			Meropenem		
	K_m, μM	k_{cat}, s^{-1}	k_{cat}/K_m, $mM^{-1}\ s^{-1}$	K_m	k_{cat}	k_{cat}/K_m	K_m	k_{cat}	k_{cat}/K_m	K_m	k_{cat}	k_{cat}/K_m
OXA-24 WT†	80	223	2,758	1,272	0.18	202	0.58	1	2,786	0.0099	0.37	37,869
	(± 15)	(± 92.9)		(± 222)	(± 0.086)		(± 0.084)	(± 0.47)		(± 0.0014)	(± 0.1)	
OXA-24 Y112A M223A	410	401	980	1,951	0.35	645	9	3	342	3	0.25	83
	(± 11)	(± 84)		(± 461)	(± 0.12)		(± 0.71)	(± 0.26)		(± 0.45)	(± 0.1)	
OXA-24 Y112A	594	274	461	3,757	0.055	197	15	5	355	1	0.22	243
	(± 60)	(± 14)		(± 816)	(± 0.019)		(± 2.20)	(± 1.21)		(± 0.15)	(± 0.05)	

*These results are the mean values of three independent experiments.
†The specific activity of the purified OXA-24 enzymes measured with 100 μM nitrocefin as substrate were 0.34, 0.39, and 0.28 μmol/min per μg of protein for WT OXA-24, double mutant OXA-24, and Y112A OXA-24, respectively.

BIOCHEMISTRY

the mutated proteins was due to a reduced affinity rather than to changes in the turnover rate (k_{cat}).

With respect to oxacillin, the activity of OXA-24 toward this antibiotic ($k_{cat}/K_m \approx 200$) was very low when compared with other oxacillinases. However, the Y112A and M223A substitutions induced significant higher increase in activity of >3-fold. In contrast, both imipenem and meropenem were readily degraded by WT OXA-24 with high catalytic efficiency (Table 2). The mutated OXA-24-Y112A and OXA-24–DM displayed weaker catalytic efficiency against carbapenems, although this effect was more drastic with meropenem (the meropenem k_{cat}/K_m ratios were 456 and 155 times lower in the OXA-24 DM and OXA-24 Y112A, respectively). Interestingly, the K_m for imipenem and meropenem was much higher in both OXA-24-Y112A and OXA-24-DM, whereas the k_{cat} remained almost identical in both the WT OXA-24 and the mutant enzymes. Although Met-223 is close to the KSG domain, the Tyr-112 and Met-223 residues lie outside of the active center, and they are not directly involved in β-lactam catalysis. Thus, the biochemical data are consistent with the structural data in that they suggest that the Tyr-112-Met-223 "hydrophobic barrier" is the main factor that dictates the biochemical properties of the OXA-24 enzyme. Indeed, no real change in the active center of the OXA-24 enzyme can be responsible for the changes in the kinetic parameters toward carbapenems because the k_{cat} values of the mutant OXA-24 enzymes with respect to meropenem were almost identical to that of the WT. However, there was a clear reduction in the k_{cat}/K_m ratio with both Y112A and DM, suggesting that in the absence of this tunnel-like entrance, carbapenems are not correctly orientated and therefore cannot gain access to the active center.

Discussion

OXA-24 is a carbapenem-hydrolyzing class D β-lactamase isolated from a multiresistant clinical isolate of *A. baumannii*, which is naturally highly resistant to carbapenem antibiotics (9). There is a worldwide increase in the resistance of bacterial pathogens to carbapenem antibiotics associated with the production of OXA-type β-lactamases (9, 12, 30). Hence, these enzymes become interesting candidates for structural studies to determine the molecular mechanism of carbapenem resistance at the atomic level. From the crystal structure of OXA-24, a plausible model for its carbapenem binding specificity has been generated. In this model, a pair of amino acid residues (Tyr-112 and Met-223) emerges that are directly related to this resistance and that confers unique structural features to a carbapenemase enzyme. The relative orientation of both key residues delimits the access to the catalytic binding-site, underlining the importance of the appropriate positioning of the antibiotic for optimal recognition (20). Furthermore, a change in the conformation of the β4-β5 loop toward the lower boundary of the cleft of the active site partially blocks the bottom part of the channel, acting like a flip lid, and this generates a hydrophobic core using the lateral chains of several nonpolar residues (Fig. 2*c*).

The docking of imipenem and meropenem within the binding site fully supports the proposed role of Tyr-112 and Met-223 in establishing specificity and yields further insight into how the β-lactam antibiotic complex is formed (Fig. 5 *a* and *b*). Notably, the substrate is visibly anchored into the tunnel-like cavity of the active site with no significant displacement of the protein side-chains. Carbapenem molecules bind through the carboxylate and the 6α-hydroxyethyl groups at the left position of the β-lactam ring (Fig. 4*c*) through two types of interactions: a strong salt-bridge contact between the carboxylate group of the antibiotic and the guanidinium moiety of Arg-261; and a hydrogen bond between the hydroxyl group of the drug and the main-chain carbonyl oxygen atom of Trp-221, as well as a favorable van der Waals interaction between the aliphatic methyl group and the nonpolar Val-130 residue. Moreover, the sulfur-containing side-chain at position 3 of the carbapenem ring

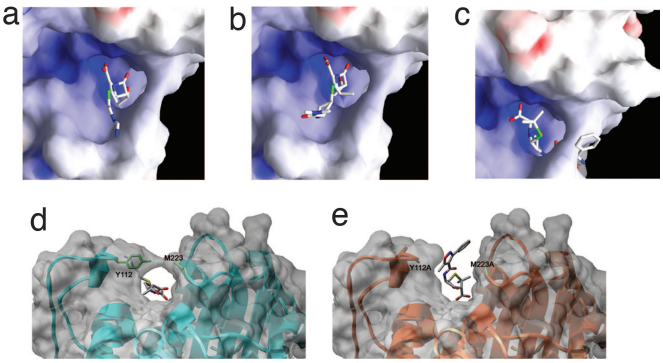

Fig. 5. The effect of point mutations on substrate selectivity. (*a* and *b*) Docking of imipenem (*a*) and meropenem (*b*) within the active site. The substrate is visibly anchored into the tunnel-like cavity of the binding site. Models of OXA-24 with carbapenems, based on the published structures (18), were manually fitted onto the active site and then subjected to energy minimization by using the CNS program (16). (*c*) Schematic representation of the active site of OXA-24 with a hypothetical oxacillin molecule. The bulk side-chain of this β-lactam antibiotic, at position 6 of the β-lactam ring, collides with the hydrophobic barrier at the tunnel-like entrance. (*d*) Important catalytic residues in the active site. The Tyr-112 residue seems to be essential for catalytic efficiency against carbapenems because it hooks the 6-α-hydroxyethyl group of these β-lactam antibiotics before catalysis. (*e*) The hypothetical active site cavity of the OXA-24 double mutant. The binding modus of oxacillin in the double mutant mimics the specific binding of isoxazolyl penicillin derivatives to the open cleft of oxacillinases (17, 19).

(aminomethylideneamino-ethyl sulfanyl of imipenem and 5-dimethylcarbamoyl pyrrolidin-2yl sulfanyl of meropenem) runs almost parallel to the active site by stacking with various residues on the hydrophobic surface of the cleft (i.e., Tyr-112, Met-114, Trp-115, and Leu-127). The derived molecular modeling interactions are consistent with some of the key features of the ligand binding properties inferred from the OXA-13-meropenem complex (18). In turn, this explains why carbapenems but not isoxazolyl penicillins such as oxacillin, with bulkier substituents at position 6 of the β-lactam ring, are specifically degraded by OXA-24 (Fig. 5*c*).

Finally, to validate the structural model and to clarify how the Tyr-112 and Met-223 residues participate in carbapenem specificity, structural mutants were constructed. Our structural and mutagenesis studies demonstrate that Tyr-112 and Met-223 are important for the carbapenemase activity of OXA-24. With carbapenems, clear imipenem and meropenem resistance was observed when WT OXA-24 was expressed in *A. baumannii*. Although substitution of Met-223 by alanine (M223A) slightly diminishes the carbapenem MIC values, the mutant Y112A significantly decreased imipenem and meropenem MIC values. When both amino acid changes were introduced in WT OXA-24 together, the imipenem MIC decreased to 4 μg/ml, whereas meropenem practically reached basal levels. Biochemical experiments also confirm the lower catalytic efficiency of the selected mutants against carbapenems. With either Y112A or the double mutant there was a clear reduction in the k_{cat}/K_m ratio, which suggests that in the absence of the characteristic tunnel-like entrance carbapenems are not correctly orientated and therefore, they cannot properly reach the active center. The role of Tyr-112 seems to be essential for catalytic efficiency against carbapenems as it hooks the 6-α-hydroxyethyl side chain of these β-lactam antibiotics (31) before catalysis (Fig. 5*d*). Interestingly, the substitution of these residues in OXA-24 confers almost a 4-fold increase in the hydrolytic activity for oxacillin, even though the activity of the WT enzyme against this β-lactam antibiotic is very low. This may be related to the abrogation of the tunnel-like entrance to the active site in the WT OXA-24, a phenomenon that is avoided when this channel is eliminated in the double mutant (Fig. 5*e*). In this respect, the binding modus of oxacillin in the double mutant mimics the way

that isoxazolyl penicillin derivatives specifically bind to the open cleft of oxacillinases (17, 19).

Furthermore, the structure-based multiple sequence alignment (see SI Fig. 7) provides additional information regarding the differences in the catalytic properties of these two members of the class D β-lactamases, oxacillinases, and carbapenemases. The determinants for substrate specificity of OXA-24 are shared by other subgroups of carbapenem-hydrolyzing class D β-lactamases (CHDLs), mainly found in *A. baumannii*, and represented by OXA-23, OXA-51, and OXA-58, which can be either plasmid- or chromosomally encoded (13). In fact, all CHDLs possess an aromatic residue (Tyr or Phe) at the position equivalent to Tyr-112 in the OXA-24 sequence, whereas the second key residue at position 223, Met in OXA-24, may accommodate either methionine or tryptophan. The amino acid similarities found in these two key residues for carbapenem-hydrolyzing enzymes are extensive enough to suggest that they are crucial for the architecture of the tunnel-like active site that permits the specific accommodation of the 6α-1R-hydroxyethyl group of carbapenems but not for antibiotics with bulkier groups at position 6 of the β-lactam ring (i.e., oxacillin, cloxacillin, and methicillin).

To our knowledge this is a previously unrecognized description of the structural and biochemical mechanisms associated with carbapenem hydrolysis in a class D carbapenemase enzyme. The findings of this study provide structural information that helps us to understand the molecular basis underlying the acquisition of carbapenem specificity and could serve as a starting point for the development of new antimicrobial agents.

Materials and Methods

Full protocols are available in *SI Text*.

Bacterial Strains and Growth Conditions. To clone the OXA-24 gene, an *A. baumannii* clinical isolate strain resistant to carbapenems that was previously reported to harbor this gene was used (RYC 52763/97; ref. 9). *E. coli* TG1 [genotype: F′ *traD36 LacI*^{q} Δ(*lacZ*)*M15*] *proA+B+*/ *supE* Δ(*hsdMmcrB*)5($r_k^-m_k^-McrB^-$) *thi* Δ(*lac-proAB*) and *E. coli* BL21 [genotype: F$^-$ *ompT HsdS*$_B$ ($r_B^-m_B^-$) *gal dcm*] were used for cloning and for the expression and purification of proteins, respectively. *A. baumannii* JC7/04 was used as a host of the different recombinant plasmids for MIC studies.

Antimicrobial Agents and Determination of MICs. Antibiotic susceptibility profiles were determined by microdilution following National Committee for Clinical Laboratory Standards criteria (32). In addition, the MICs for the following antibiotics were confirmed by the E test (AB Biodisk, Solna, Sweden): ampicillin (AM), imipenem (IP), and meropenem (MP).

Site-Directed Mutagenesis and Cloning Procedures. PCR was used to amplify the gene coding for WT and mutated oxa-24 genes (oxa-24–Y112A, oxa-24–M223A, and oxa-24 DM). These WT OXA-24 and mutated genes were then cloned into the pAT-RA plasmid, a previously described *E. coli–A. baumannii* shuttle plasmid (at the SmaI and EcoRI restriction sites), under the control of the CTX-M-14 β-lactamase gene promoter.

Purification and Kinetic Experiments. The WT OXA-24 and mutated genes were subcloned into pGEX-6p-1 (BamHI and EcoRI restriction sites) to generate a fusion protein between GST and the OXA-24 genes lacking the signal peptide. The β-lactamase was then purified to homogeneity following the manufacturer's instructions for the GST Gene Fusion System (Amersham Pharmacia Biotech, Europe GmbH, Barcelona, Spain). Kinetic experiments were performed as described (33).

Crystallization, Data Collection, Structure Determination, and Refinement. Crystals of recombinant OXA-24 were obtained in 2 M $(NH_4)_2SO_4$ buffered with 100 mM sodium acetate (pH 4.5). Data were collected at the European Synchrotron Radiation Facility (Grenoble, France) beamline BM16 by using a single frozen crystal (100 K) (see SI Table 3). Data were processed and refined as described in *SI Text*.

We thank the staff of beamline BM16 at the European Synchrotron Radiation Facility for their support, C. Fernández-Cabrera for excellent technical assistance, G. Rivas for ultracentrifugation studies, and P. Grooves and M. Sefton for critical reading of the manuscript. This work was supported by Grant BFU2005-05055 from the Spanish Ministry of Science; Grant PGIDI4BTF916028PR from Dirección Xeral I+D, Xunta de Galicia; and Grants PI040514, PI061368, and RD06/0008 from the Fondo de Investigaciones Sanitarias. E.S. holds a fellowship from the Spanish Ministry of Science. A.B. is a recipient of a scholarship from the Sociedad Española de Enfermedades Infecciosas y Microbiología Clínica.

1. Lee W, McDonough MA, Kotra L, Li ZH, Silvaggi NR, Takeda Y, Kelly JA, Mobashery S (2001) *Proc Natl Acad Sci USA* 13:1427–1431.
2. Frère JM (1995) *Mol Microbiol* 16:385–395.
3. Ambler RP (1980) *Phil Trans R Soc London B* 289:321–331.
4. Majiduddin FK, Materon IC, Palzkill TG (2002) *Int J Med Microbiol* 292:127–137.
5. Ledent P, Raquet X, Joris B, Van Beeumen J, Frère JM (1993) *Biochem J* 292:555–562.
6. Afzal-Shah M, Livermore DM (1998) *J Antimicrob Chemother* 41:576–577.
7. Poirel L, Marque S, Heritier C, Segonds C, Chabanon G, Nordmann P (2005) *Antimicrob Agents Chemother* 49:202–208.
8. Naas T, Levy M, Hirschauer C, Marchandin H, Nordmann P (2005) *J Clin Microbiol* 43:4826–4829.
9. Bou G, Oliver A, Martinez-Beltran J (2000) *Antimicrob Agents Chemother* 44:1556–1561.
10. Brown S, Young HK, Amyes SG (2005) *Clin Microbiol Infect* 11:15–23.
11. Girlich D, Naas T, Nordmann P (2004) *Antimicrob Agents Chemother* 48:2043–2048.
12. Afzal-Shah M, Woodford N, Livermore DM (2001) *Antimicrob Agents Chemother* 45:583–588.
13. Walther-Rasmussen J, Høiby N (2006) *J Antimicrob Chemother* 57:373–383.
14. Livermore DM (2002) *Curr Opin Investig Drugs* 3:218–224.
15. Sun T, Nukaga M, Braswell EH, Knox JR (2003) *Protein Sci* 12:82–91.
16. Brünger AT, Adams PD, Clore GM, DeLano WL, Gros P, Grosse-Kunstleve RW, Jiang JS, Kuszewski J, Nilges M, Pannu NS, *et al.* (1998) *Acta Crystallogr D* 54:905–921.
17. Paetzel M, Danel F, de Castro L, Mosimann SC, Page MGP, Strynadka NCJ (2000) *Nat Struct Biol* 7:918–925.
18. Pernot L, Frénois F, Rybkine T, L'Hermite G, Petrella S, Delettré J, Jarlier V, Collatz E, Sougakoff W (2001) *J Mol Biol* 310:859–874.
19. Maveyraud L, Golemi D, Kotra LP, Tranier S, Vakulenko S, Mobashery S, Samama JP (2000) *Structure Fold Des* 8:1289–1298.
20. Macheboeuf P, DiGuilmi AM, Job V, Vernet T, Dideberg O, Dessen A (2005) *Proc Natl Acad Sci USA* 102:577–582.
21. Contreras-Martel C, Job V, Di Guilmi AM, Vernet T, Dideberg O, Dessen A (2006) *J Mol Biol* 355:684–696.
22. Jelsch C, Mourey L, Masson J-M, Samama J-P (1993) *Proteins* 16:364–383.
23. Frère JM, Dubus A, Galleni M, Matagne A, Amicosante G (1999) *Biochem Soc Trans* 27:58–63.
24. Wilke MS, Lovering AL, Strynadka NCJ (2005) *Curr Op Microbiol* 8:525–533.
25. Ghuysen JM (1994) *Trends Microbiol* 2:372–380.
26. Poole K (2004) *Cell Mol Life Sci* 61:2200–2223.
27. Brown S, Amyes SGB (2005) *Clin Microbiol Infect* 11:326–329.
28. Strynadka NCJ, Adachi H, Jensen SE, Johns K, Sielecki A, Betzel C, Sutoh K, James MN (1992) *Nature* 359:700–705.
29. Marrero A, Mallorqui-Fernandez G, Guevara T, Garcia-Castellanos R, Gomis-Ruth FX (2006) *J Mol Biol* 361:506–521.
30. Donald HM, Scaife W, Amyes SG, Young HK (2000) *Antimicrob Agents Chemother* 44:196–199.
31. Moellering RC, Eliopoulos GM, Sentochnik DE (1989) *J Antimicrob Chemother* 24(Suppl A):1–7.
32. National Committee for Clinical Laboratory Standards (2003) *Approved Standard M7–A6: Methods for Dilution Antimicrobial Susceptibility Tests for Bacteria That Grow Aerobically* (National Committee for Clinical Laboratory Standards, Wayne, PA).
33. Hujer KM, Hamza NS, Hujer AM, Perez F, Helfand MS, Betherl CR, Thomson JM, Anderson VE, Barlow M, Rice LB, *et al.* (2005) *Antimicrob Agents Chemother* 49:2941–2948.